Hysteresis Phenomena Behind Freeway Bottlenecks

Alexander Hammerl, Ravi Seshadri, Thomas Kjær Rasmussen, Otto Anker Nielsen[1]

[1]Department of Transport, Technical University of Denmark

Short summary

This study aims to improve the understanding of hysteresis phenomena in Network Macroscopic Fundamental Diagrams (NMFDs) and Network Exit Functions (NEFs) during rush hours. We employ the LWR model based on trapezoidal boundary conditions upstream of a discontinuous bottleneck to analyze the time-dependent relationship between traffic accumulation and trip completion rate and average flow in urban traffic networks. The methodology includes a theoretical analysis supported by numerical experiments to approximate rush hour-specific traffic behavior. The study links the relationship between inhomogeneous vehicle distribution in traffic networks and hysteresis loops in MFD relationships to measurable traffic flow quantities for the first time. The main conclusions indicate the presence of hysteresis loops in flow- and outflow-MFDs. The study contributes to traffic flow modeling by offering insights into the effects of congestion distribution and network topology on traffic performance.
Keywords: traffic flow theory, hysteresis, bottlenecks

1 Introduction

Godfrey (1969) appears to be the first author to postulate a strictly functional, uni-modal relationship between average flow and density in urban traffic networks two variables. After traffic flow theory C. Daganzo & Geroliminis (2008) and empirical data Geroliminis & Daganzo (2008) have more recently confirmed the existence of such relationships, their estimation and analysis have gained considerable popularity. Such relationships are commonly referred to as Network Macroscopic Fundamental Diagrams (NMFDs) or flow-MFDs. A similar relationship, known as the Network Exit Function (NEF) or outflow-MFD, has also been demonstrated between trip completion rate and average density C. Daganzo (2007).
In a recent review paper, Johari et al. (2021) categorize the requirements for the existence of MFDs as follows: demand homogeneity, road homogeneity, and control homogeneity. In particular, the assumption of demand and road homogeneity is only rarely possible without restrictions in transportation network modeling. Buisson & Ladier (2009) show that the inhomogeneity of density within a network during rush hour can influence the relationship between traffic flow and density in such a way that clockwise hysteresis loops may form. Next, Mazloumian et al. (2010) and Yi et al. (2010) and later Mahmassani et al. (2013) and Leclercq et al. (2015) confirmed that congestion distribution influences the emergence of NMFD hysteresis loops. The significance of congestion distribution for the MFD's shape and scatter has sparked interest in how this parameter can be appropriately addressed in macroscopic network modeling (e.g. Yi & Geroliminis (2012)).
Other sources attribute the occurrence of hysteresis loops to the topology of the respective road networks. As early as Buisson & Ladier (2009) and Yi et al. (2010), it was indicated that more pronounced hysteresis effects are to be expected in freeway networks. Geroliminis & Sun (2011), Saberi & Mahmassani (2012), and Saberi & Mahmassani (2013) provide a detailed discussion about freeway NMFDs.
In contrast to previously described macroscopic modeling approaches, the theory by Lighthill, Whitham Lighthill & Whitham (1955), and Richards Richards (1956) (LWR) assumes that traffic flow and density are locally related in a concave functional relationship, known as the fundamental diagram. The LWR theory is well-suited for analyzing local traffic jam dynamics, but its application in larger networks is prohibitively resource-intensive. Existing mesoscopic analyses of traffic jams behind bottlenecks within the LWR framework do not account for the characteristic congestion buildup and subsequent dissipation of traffic corridors during peak hours. Jin (2017) analyzes

traffic jam formation behind bottlenecks modeled as Riemann problems in various LWR-derived theories. Newell (1999) describes a gradual increase in congestion behind continuous bottlenecks for two specific shapes of the fundamental diagram (triangular and parabolic) but does not address congestion reduction. Kerner (2002) develops an empirical theory for traffic movements behind bottlenecks. The aim of this article is to improve the understanding of the causes of hysteresis in NMFDs and NEFs. To achieve this, rush hour-specific traffic behavior is approximated as a boundary value problem with trapezoidal demand upstream of a discontinuous bottleneck.

2 Methodology

The specific formulation of the model follows C. F. Daganzo (1995). If traffic flows in the direction of increasing x and we take $x_1 > x_2$, then

$$\frac{\partial}{\partial t}\int_{x_1}^{x_2} k(x,t)\,dx + q(x_2,t) - q(x_1,t) = 0. \tag{1}$$

and

$$q(x,t) = Q(k(x,t)), \tag{2}$$

where Q is a differentiable, non-negative function that is zero for $k = 0$ and $k = k_j$. The cumulative flow $N(x,t)$ is defined such that its negative partial derivative with respect to space yields the traffic density $k(x,t)$, and its partial derivative with respect to time yields the traffic flow $q(x,t)$:

$$-\frac{\partial N}{\partial x}(x,t) = k(x,t), \tag{3}$$

$$\frac{\partial N}{\partial t}(x,t) = q(x,t). \tag{4}$$

If k is differentiable, 1 can be expressed as

$$\frac{\partial k}{\partial t} + \frac{\partial q}{\partial x} = 0, \tag{5}$$

for $x_2 \to x_1$. If k has a jump discontinuity at (x,t), the conservation principle specifies that the velocity of the jump, u, is:

$$u = \frac{[q]}{[k]} = \frac{[Q(k)]}{[k]}, \tag{6}$$

where brackets denote the change in the enclosed variable across the discontinuity.
We assume a trapezoidal shape of the flow on the upstream boundary as a function of time, on a link that is otherwise empty at $t = 0$. That is,

$$q(0,t) = \begin{cases} q_b + (q_p - q_b)\cdot t, & \text{for } 0 \le t \le t_{pb}, \\ q_p, & \text{for } t_{pb} \le t \le t_{pe}, \\ q_p - \frac{(q_p - q_e)}{(t_e - t_{pe})}\cdot(t_e - t), & \text{for } t_{pe} \le t \le t_e, \\ q_e, & \text{for } t_e \le t \le \infty. \end{cases} \tag{7}$$

Traffic flows through a link of length l with a bottleneck with maximum capacity q_{bn} at its downstream end. $k_{\text{bn,c}}$ is defined as the highest density k for which $q(k) = q_{\text{bn}}$, while $k_{\text{bn,u}}$ is defined as the lowest density satisfying the same condition. Let $A(t)$ denote the total number of vehicles on the link at time t, referred to as the accumulation. Let $\bar{q}(t)$ represent the average flow on the link at time t. Finally, let $P(t)$ symbolize the flow at the downstream end at time t. It is assumed that the upstream boundary conditions always result in a queue at the bottleneck. Additionally, we assume that the tail of the queue never exceeds the physical capacity of the link.
The set of characteristic lines, represented as straight lines in space-time, is defined by the equation $\frac{dq}{dk}(0,t_0)\cdot(t - t_0)$ for every t_0. The trajectory of the tail of the queue in space-time is denoted by $\psi(t)$.

Lemma 2.1. *For every point (x,t) satisfying $x < \psi(t)$ which is reached by at least one characteristic curve, the physically correct characteristic is the latest emanating one.*

Proof (Sketch). Consider a point (x,t) intersected by at least two characteristics. Let t^+ be the latest time instant a characteristic reaching (x,t) emanates from the upstream boundary, with c^+

denoting the corresponding characteristic curve. Intersection of two characteristic lines implies the later emanating characteristic, starting at a time $t^- > t_{pe}$, occurs when the boundary demand decreases. Consequently, for all points (x^-, t), where $x^- \leq x$, characteristics reaching these points have lower associated densities than that of c^+. Given the weak differentiability of $N(x,t)$ with respect to x, this implies the desired result. □

Lemma 2.2. *Denote as $\hat{t}$ the time instant at which the phsically correct characteristic reaching psi(t) at t starts from the upstream boundary.The trajectory of the tail of the queue in space-time, $\psi(t)$, is then given by the formula:*

$$\psi(t) = l - \left(v(k(0,t_0)) - \frac{dq}{dk}(0,\hat{t})\right) \cdot k(0,t_0(\psi(t),t)) - N_0 + q_b \cdot (t - t_b), \tag{8}$$

Proof (Sketch). The proof leverages the equivalence of the integration paths for $N(x,t)$. Specifically, the first path from $(0,0)$ to $(l,0)$, then to (l,t), and finally to $(\psi(t),t)$, and the second path from $(0,0)$ directly to $(0,\hat{t})$, and then to $(\psi(t),t)$. By equating the integrals along these paths and solving for $\psi(t)$, the desired formula is obtained. □

3 Results and discussion

Proposition 3.1. *The time-dependent relationship between $A(t)$ and $P(t)$ is characterized by an anti-clockwise hysteresis loop, described by the following sequence of phases:*

1. *From $t = 0$ to $t^{(1)}_{P,max}$, both $A(t)$ and $P(t)$ increase, tracing curve $\bar{A}$ up to the point $(\bar{k}_1, q_{bn})$.*
2. *Between $t^{(1)}_{P,max}$ and $t_{A,max}$, $P(t)$ remains constant at q_{bn} while $A(t)$ increases to $\bar{k}_{max}$.*
3. *From $t_{A,max}$ to $t^{(2)}_{P,max}$, $P(t)$ stays constant, but $A(t)$ decreases to $\bar{k}_2 < \bar{k}_1$.*
4. *Finally, in the interval $t^{(2)}_{P,max}$ to $t_{eq,end}$, the relationship moves along the decreasing curve $\bar{B}$ from $(\bar{k}_2, q_{bn})$ to $(k_{bn,c} \cdot l, q_e)$, with $\bar{B}(\bar{k}) > \bar{A}(\bar{k})$ for all $\bar{k} \in [k_{bn,c}, \bar{k}_2]$.*

Proof. Proof(Sketch) We prove each part of the proposition as follows:

1. *From $t = 0$ to $t^{(1)}_{P,max}$*: Characteristics originating from the upstream boundary do not intersect during this period, and the flow associated with each characteristic rises with its emanation time. Consequently, as each point on the downstream boundary corresponds to precisely one characteristic, the property of increasing $\bar{A}$ is evident.
2. *Between $t^{(1)}_{P,max}$ and $t_{A,max}$, and from $t_{A,max}$ to $t^{(2)}_{P,max}$*: The exit flow equals q_bn iff $\psi(t) < l$. Characteristic line c_1, initiating queuing at the downstream, has flow $> q_{bn}$; c_2, ending queuing, has flow $< q_{bn}$. Given c_1 arises with increasing upstream flows and c_2 with decreasing ones, and since accumulation is the integral of upstream flow over time, accumulation is greater at the queue's start than its end.
3. *Finally, in the interval $t^{(2)}_{P,max}$ to $t_{eq,end}$*: The proof follows the arguments made in the first two parts.

□

Proposition 3.2. *The time-dependent relationship between $A(t)$ and $\bar{q}(t)$ forms a clockwise hysteresis loop characterized by three phases:*

1. *From $t = 0$ to $t = t_{\hat{q}_{\max}}$, $A(t)$ increases with $\hat{q}(t)$, moving northeast along curve A.*
2. *From $t = t_{\hat{q}_{\max}}$ to $t = t_{A_{\max}}$, the relationship transitions along curve B, moving southeast as $\hat{q}(t)$ decreases while $A(t)$ continues to increase, reaching its maximum.*
3. *Beyond $t = t_{A_{\max}}$, as time approaches infinity, the curve moves southwest, indicating a decrease in both $A(t)$ and $\hat{q}(t)$, eventually intersecting curve A again.*

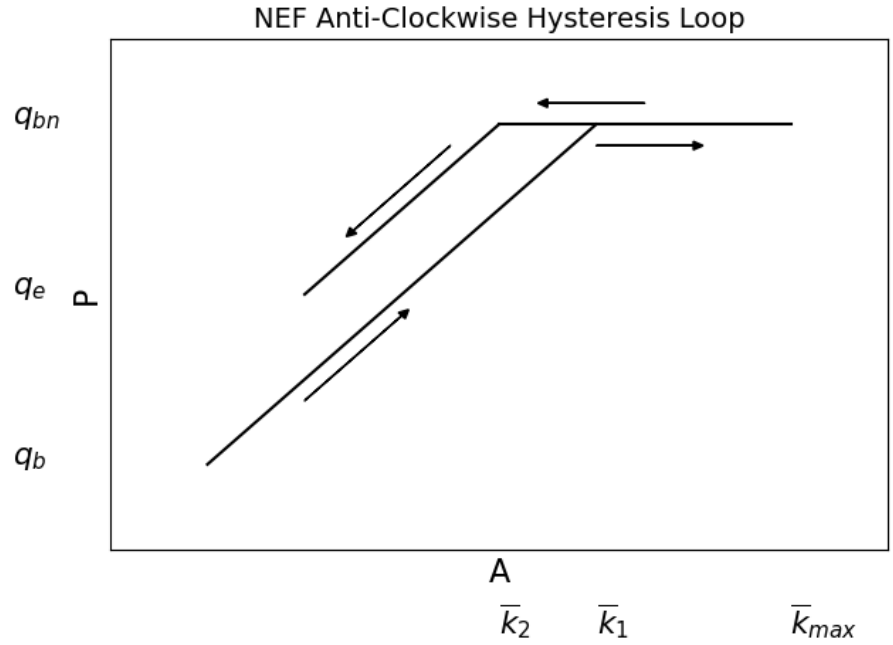

Figure 1: Time-dependent relationship between accumulation and trip completion rate. The directional arrows symbolize progression of time.

Proof (Sketch). For this abstract, we demonstrate the proposition of the lemma for time instants t for which $\psi(t) < l$, i.e. those where there is an active queue. We do so by showing $A(t_1) = A(t_2)$ with $t_2 > t_1$ implies $\bar{q}(t_1) > \bar{q}(t_2)$. The growth behavior of $\psi(t)$ requires that, for $A(t_1) = A(t_2)$ to be true, $\psi(t_1) > \psi(t_2)$. We can conclude that the accumulation within the queue at each instant, denoted $A_q(t)$, is higher at t_2: $A_q(t_1) < A_q(t_2)$. Consequently, the reverse relationship has to hold for the accumulation upstream of the queue, denoted $A_u(t)$ at both time instants: $A_q(t_1) < A_q(t_2)$, which implies that the average flow upstream of the queue is higher at time instant t_1. Since, however, the average flow within the queue is uniform at q_{bn} at both time instants, it follows that $\bar{q}(t_1) > \bar{q}(t_2)$. □

Finally, we present simulated examples to illustrate the hysteresis effects within the framework of a numerical approximation in the Cell Transmission Model (CTM). The simulations cover three hours, employing a triangular fundamental diagram to propagate traffic flow. This diagram is characterized by a free-flow speed of 60, a critical density of 40, and a jam density of 160. We conducted simulations for two distinct scenarios of the boundary value problem, characterized by the following boundary flows:
For a high demand scenario:

$$q_{high}(0,t) = \begin{cases} 20 + 30t & \text{if } 0 \le x \le \frac{2}{3}, \\ 40 & \text{if } \frac{2}{3} \le x \le 1, \\ 40 - 30 \cdot (t-1) & \text{if } 1 \le x \le 2. \end{cases}$$

And for a low demand scenario:

$$q_{low}(0,t) = \begin{cases} 20 + 30t & \text{if } 0 \le x \le \frac{1}{3}, \\ 30 & \text{if } \frac{1}{3} \le x \le \frac{2}{3}, \\ 40 - 30 \cdot (t-1) & \text{if } \frac{2}{3} \le x \le 1\frac{2}{3}, \\ 10 & \text{if } 1\frac{2}{3} \le x \le 3. \end{cases}$$

The outcomes of these simulations are depicted in Figures 2 and 3.
Our analysis reveals that the magnitude of hysteresis appears to be uniform across different peak boundary demands for Network exit functions. This observation may be attributed to how an increase in peak demand is achieved between the simulated instances, namely by extending the length of the intervals of increase instead of their slope. Consequently, this approach does not alter the asymmetry in the spatial distribution of vehicles during the transition from low to high

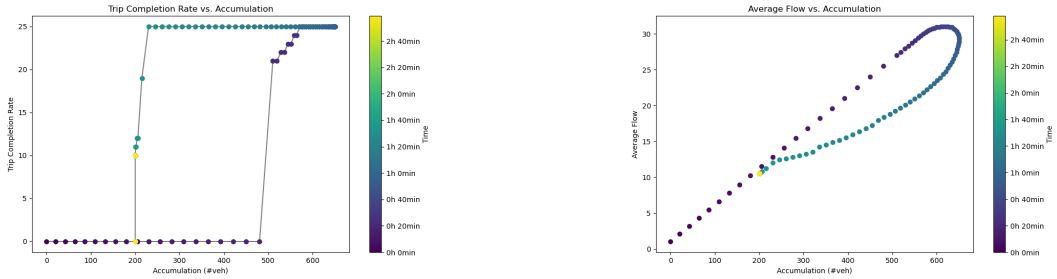

Figure 2: Low demand

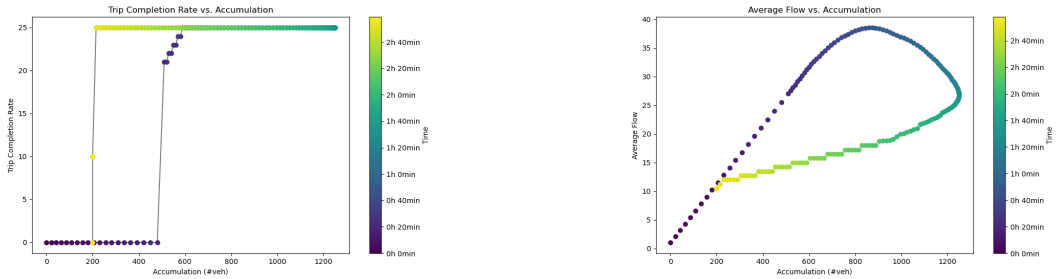

Figure 3: High demand

demand. Alternatively, had the increase in peak demand been realized through a steeper slope of the boundary value curve, we would expect a greater degree of hysteresis in scenarios of high demand.

Regarding the relationship between average flow and vehicle accumulation, our findings indicate a notable increase in hysteresis concurrent with the rise in peak demand. This observation aligns with the theoretical discussions presented in the proof of Proposition 3.2. The logic underpinning this phenomenon suggests that higher demands lead to longer queues (i.e., lower values of $\psi(t)$), thereby exacerbating the asymmetry in vehicle distribution at two distinct time points with identical accumulations.

4 Conclusions

Our mathematical model offers a new method to analyze hysteresis factors at the corridor level, showing through theoretical analysis that our predictions of hysteresis behavior match empirical data. This approach allows for identifying the shapes and sizes of hysteresis loops from traffic flow data, deepening our understanding of hysteresis in traffic systems. This understanding is based on the significant impact of vehicles' time-varying spatial distribution, with our model shedding light on these patterns. Specifically, we observe that counterclockwise hysteresis loops in the exit function result from vehicles being closer to their destinations during congestion easing, whereas clockwise loops in the Fundamental Diagram come from tighter vehicle clustering in such phases, slowing average speeds. Despite seeming obvious, this area's lack of systematic study has led to its varied representation in macroscopic traffic analyses. For example, Gayah & Daganzo (2011) notes decreased exits during congestion, contrasting with Geroliminis & Sun (2011), which assumes unchanged exit functions in networks with NMFD hysteresis. Our framework enables detailed analysis of hysteresis' responsiveness to different factors, essential for improving traffic flow models.

References

Buisson, C., & Ladier, C. (2009). Exploring the impact of homogeneity of traffic measurements on the existence of macroscopic fundamental diagrams. *Transp. Res. Rec.*, 127–136.

Daganzo, C. (2007). Urban gridlock: macroscopic modeling and mitigation approaches. *Transp. Res. Part B*, *41*, 49–62.

Daganzo, C., & Geroliminis, N. (2008). An analytical approximation for the macroscopic fundamental diagram of urban traffic. *Transp. Res. Part B Methodol.*, *42*, 771–781.

Daganzo, C. F. (1995). Requiem for second-order fluid approximations of traffic flow. *Transportation Research Part B: Methodological*, *29B*(4), 277–286.

Gayah, V. V., & Daganzo, C. F. (2011). Clockwise hysteresis loops in the macroscopic fundamental diagram: An effect of network instability. *Transportation Research Part B*, *45*, 643–655.

Geroliminis, N., & Daganzo, C. (2008). Existence of urban-scale macroscopic fundamental diagrams: some experimental findings. *Transp Res Part B*, *42*, 759–770.

Geroliminis, N., & Sun, J. (2011). Hysteresis phenomena of a macroscopic fundamental diagram in freeway networks. In *Proc. soc. behav. sci.* (Vol. 17, pp. 213–228).

Godfrey, J. (1969). The mechanism of a road network. *Traffic Eng. Control*, *11*, 323–327.

Jin, W.-L. (2017). Kinematic wave models of lane-drop bottlenecks. *Transportation Research Part B*, *105*, 507–522.

Johari, M., Keyvan-Ekbatani, M., Leclercq, L., Ngoduy, D., & Mahmassani, H. (2021). Macroscopic network-level traffic models: bridging fifty years of development toward the next era. *Transp. Res. Part C Emerg. Technol.*, *131*, 103334.

Kerner, B. S. (2002). Empirical macroscopic features of spatial-temporal traffic patterns at highway bottlenecks. *Physical Review E*, *65*.

Leclercq, L., Parzani, C., Knoop, V., Amourette, J., & Hoogendoorn, S. (2015). Macroscopic traffic dynamics with heterogeneous route patterns. *Transp. Res. C*, *59*, 292–307.

Lighthill, M., & Whitham, G. (1955). On kinematic waves ii. a theory of traffic flow on long crowded roads. *Proc. R. Soc. London. Ser. A. Math. Phys. Sci.*, *229*, 317–345.

Mahmassani, H., Saberi, M., & Zockaie, A. (2013). Urban network gridlock: Theory, characteristics, and dynamics. *Transp. Res. C*, *36*, 480–497.

Mazloumian, A., Geroliminis, N., & Helbing, D. (2010). The spatial variability of vehicle densities as determinant of urban network capacity. *Phil. Trans. R. Soc. A*, *368*(1928), 4627–4647.

Newell, G. F. (1999). Flows upstream of a highway bottleneck. In *14th international symposium on transportation and traffic theory.*

Richards, P. (1956). Shock waves on the highway. *Oper. Res.*, *4*, 42–51.

Saberi, M., & Mahmassani, H. (2012). Exploring properties of networkwide flow–density relations in a freeway network. *Transp. Res. Rec.*, *2315*(1), 153–163.

Saberi, M., & Mahmassani, H. (2013). Hysteresis and capacity drop phenomena in freeway networks: empirical characterization and interpretation. *Transp. Res. Rec.*, *2391*(1), 44–55.

Yi, Y., Daamen, W., Hoogendoorn, S., Hoogendoorn-Lanser, S., & Qian, X. (2010). Investigating the shape of the macroscopic fundamental diagram using simulation data. *Transp. Res. Record: J. Transp. Res. Board*(2161), 40–48.

Yi, Y., & Geroliminis, N. (2012). On the spatial partitioning of urban transportation networks. *Transp. Res. B*, *46*(10), 1639–1656.